PAPER

Check for updates

Effects of molecular ordering on circularly polarized emission from a twisted mesogenic conjugated polymer†

Dong-Min Lee, Gi-Eun Kim, Jae-Hoon Kim* and Chang-Jae Yu 🕩 *

Circularly polarized (CP) photoluminescence and electroluminescence (EL) generated from the emitting layer can improve the light efficiency of a commercialized organic light-emitting display. High CP emission is generated from the twisted configuration of a mesogenic conjugated polymer. However, the effect of the material and device parameters on the degree of CP emission, defined by the dissymmetry g factor, has not yet been fully studied. Through carefully investigating various parameters under various experimental conditions, it was found that the degree of CP emission can be expressed as the quadratic equation of the order parameter (S). Furthermore, a considerable degree of CP emission ($g = 0.37$ in the EL process) can be measured even when the order parameter was zero. Such results imply that the twisted stacks even at a random orientation are predominant rather than the formation of a uniform orientation to generate CP light. Also, the anti-reflection condition, required in conventional organic light-emitting diodes to eliminate the reflection of ambient light from a metal cathode, is still maintained since there is no retardation in the ambient light for $S = 0$ while emitting CPEL, which leads to an enhancement of luminance efficiency by about 18.5%. It is expected that these results, discussed herein, pave the way toward understanding the mechanism of CP emission and enhancing the performance of the CP emission.

Introduction

The emission of circularly polarized (CP) light from mesogenic conjugated polymers has attracted much attention in technical applications such as displays, optical information storage systems, and chirality sensors.[1–5] In particular, direct CP emission from the emitting layers of organic light-emitting diodes (OLEDs) would facilitate the enhancement of luminance efficiency since a circular polarizer is generally used to eliminate the reflection of ambient light from metallic cathodes in conventional OLEDs.[6,7] It should be noted that the circular polarizer extracts only half of the light emitted from an OLED panel, which results in a 50% loss of luminance efficiency even before considering the other inherent losses such as internal reflection and absorption in an multi-stacked OLED.[8] However, direct CP emission from an emitting layer (EML) with the same

handedness as that provided by a circular polarizer would increase luminance efficiency (see Fig. S1 in the ESI†).

The enhancement of light extraction efficiency by direct CP emission is related to the degree of CP emission, defined by the dissymmetry g factor $g = 2(I_L - I_R)/(I_L + I_R)$. Here, I_L and I_R represent the intensities of left-handed CP (LHCP) light and right-handed CP (RHCP) light, respectively. The twisted stacks of mesogenic luminophores induced by a chiral dopant or surface treatment of the EML lead to a high dissymmetry g factor.[4,7,9–13] Here, linearly polarized (LP) light emitted from locally aligned conjugate polymers experiences birefringence passing through the twisted stacks of the mesogenic polymer and the CP light is extracted. In the twisted stacks of mesogenic luminophores, the dissymmetry g factor was governed by several parameters such as the total twisted angle, birefringence, and the location of the electron–hole recombination zone (the emission zone) within the EML.[7,11–14] However, the twisted mesogenic luminophores on the well-controlled alignment layer produce the phase retardation of ambient light and consequently break the anti-reflection condition to eliminate reflection of ambient light.[7] Furthermore, the relationship between the dissymmetry factor and molecular ordering, directly related to the phase retardation of an EML, has not been fully analysed yet.

Department of Electronic Engineering, Hanyang University, 222 Wangsimni-ro, Seongdong-gu, Seoul 04763, Republic of Korea. E-mail: jhoon@hanyang.ac.kr, cjyu@hanyang.ac.kr

In this work, we systematically analyse the dissymmetry factors with respect to molecular ordering based on the Mueller matrix analysis of photoluminescence (PL) and electroluminescence (EL) processes in a twisted EML. To produce twisted configurations with different total twisted angles, different concentrations of chiral agents were doped into a mesogenic luminophore. The mesogenic luminophore was aligned by the rubbing method[15,16] and its molecular ordering on the EML surface was controlled by varying the azimuthal anchoring strength, governed by the contact distance, which is the rubbing depth of the alignment layer for the EML with a rubbing cloth. The birefringent values and molecular order parameters of the EML without the chiral dopant were evaluated according to the contact distance. The dissymmetry g factors of the PL and EL devices with various total twisted angles (controlled by concentrations of the chiral dopant) and various order parameters (controlled by the contact distance) were experimentally measured and theoretically calculated based on the Mueller matrix analysis of the continuously twisted mesogenic sublayers, where the LP light emitted from the locally aligned mesogenic sublayer experiences birefringence passing through the twisted sublayers.[7,11–14] The degree of LP light emitted from a certain mesogenic sublayer is governed by the order parameter which is controlled by the contact distance. That is, the degree of LP emission increases with the increasing order parameter. From the relationship between the experimentally measured g factors, produced by the twisted stacks with partially ordered luminophores, and the theoretically calculated g factors, produced by the twisted stacks with perfectly ordered luminophores, we propose that the dissymmetry g factor is proportional to the square of the order parameter of the mesogenic luminophores in the twisted configuration. Also, we achieved a considerable g factor ($g_{EL} = 0.37$ in the EL process) even at an order parameter of zero satisfying the anti-reflection condition to eliminate the reflection of ambient light. This result, discussed herein, may help enhancing the performance of applications based on circular polarization, including OLEDs.

Experimental section

Device fabrication

Fig. 1 shows the schematic diagrams of PL and EL emissions in the twisted stacking structures of the mesogenic conjugated polymer with a chiral dopant. The conjugated polymer, poly(9,9-di-n-octylfluorenyl-2,7-diyl)-alt-(benzo[2,1,3]thia-diazol-4,8-diyl) (F8BT from Sigma-Aldrich) and the chiral dopant, R5011 (Merck), were used as an emitting layer.[7,14] R5011 produces a twisted stacking structure of the mesogenic polymer with right-handedness due to its high helical twisting power (HTP).[7,14] Indium-tin-oxide (ITO) substrates with a sheet resistance of about 20 Ω sq^{-1} were cleaned by ultra-sonication with deionized water and an alkali detergent at 60 °C for 60 min. Copper phthalocyanine (CuPc from Lumtec) served as a 2 nm-thick hole injection layer (HIL) was deposited on the ITO substrates under a high-vacuum of 6×10^{-6} torr by thermal evaporation.
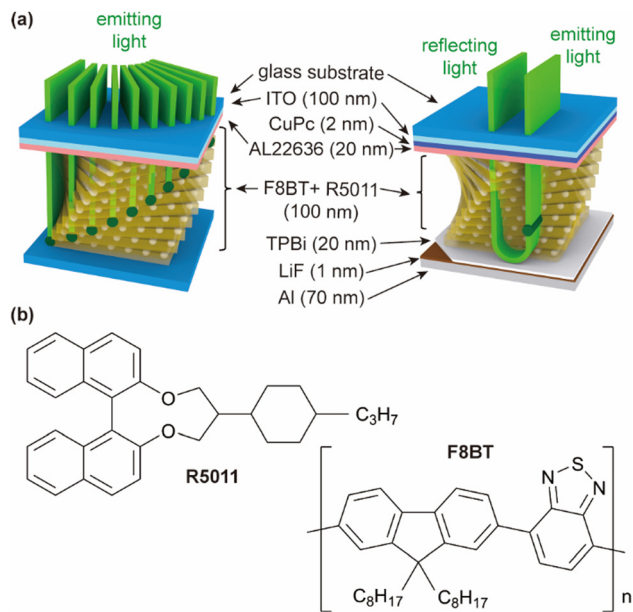

Fig. 1 (a) Schematic diagrams of PL and EL emissions in the twisted stacking of F8BT. (b) Chemical structures of R5011 and F8BT.

To control the ordering of the EML alignment, a polyimide-type (PI) alignment layer of AL22636 (from JSR) was spin-coated at 3000 rpm for 20 s, followed by 1000 rpm for 10 s on the CuPc layer and imidized via soft baking at 100 °C for 10 min and hard baking at 210 °C for 60 min. The PI surface with a 20 nm thickness was rubbed using a rubbing machine (RMS-50-M from Nam Il Optical Instruments Co.) having a 65 mm diameter roller covered with a cotton cloth. The substrate was translated at a constant speed of 50 mm s^{-1} and passed under the roller rotating at 1000 rpm. To investigate the effect of the PL and EL g factors on EML ordering, we adjusted the contact distance between the rubbing roller and the PI layer from 0 to 40 μm with 10 μm intervals. The F8BT/R5011 mixtures with different concentrations of R5011 (6, 9, and 12 wt%) were dissolved in toluene and spin-coated (at 1000 rpm for 10 s and 3000 rpm for 20 s) with 100 nm thickness on the rubbed PI layer, followed by thermal annealing at their mesogenic temperature of 160 °C for 10 min (see Fig. S2 in the ESI†). For EL devices, 2,2′,2″-(1,3,5-benzinetriyl)-tris(1-phenyl-1-H-benzimidazole) (TPBi from Lumtec) with 20 nm as a hole blocking layer (HBL), LiF (Lumtec) with 1 nm as an electron injection layer (EIL), and Al (from iNexus) with 70 nm as a cathode were sequentially deposited under a high-vacuum of 6×10^{-6} torr by thermal evaporation. To avoid exposure to oxygen and humidity, all fabricated samples were encapsulated with glass and UV curable resin (NOA 68 from Norland Products) under a nitrogen atmosphere in a glove box.

Device characterization

Luminous intensities parallel and perpendicular to the rubbing direction of the PI layer were measured under a linear polarizer using a spectroradiometer (SR-UL 1R from TOPCON) to observe the linearly polarized (LP) photoluminescence (LPPL). The CP photoluminescence (CPPL) and the CP electroluminescence

(CPEL) were measured under a circular polarizer consisting of a quarter-wave-plate (QWP) at 546 nm and a linear polarizer using a spectroradiometer. All the luminous properties of EL devices were characterized under applied voltages of 10–13 V with a power supply (PPE-3323 from GW Instek). Using a photoelastic modulator (PEM) method consisting of the PEM (PEM-100 from Hinds Instruments) and lock-in amplifier (SR830 from Stanford Research System),[17] the optical retardation of the F8BT film was measured. The twist angle of the F8BT film was determined by the measurement of the Stokes parameters of the transmitted light.[14,18] The microscopic texture and the surface morphology were observed using a polarized microscope (E600W POL from Nikon) and an atomic force microscope (AFM) (XE-100 from Park System).

Results and discussion

Mesogenic conjugated polymers at mesogenic temperature are preferentially aligned in the promoted direction by surface treatment such as the rubbing process. In a microscopic model, the orientational order of the mesogenic molecules is expressed by the order parameter, $S = \langle P_2(\cos\theta) \rangle = \langle (3\cos^2\theta - 1)/2 \rangle$, given by averaging the individual orientational deviations of the molecules from the promoted direction. Here, P_2 denotes the second-order coefficient of a Legendre polynomial.[19] However, the optical phenomena such as optical anisotropy and phase retardation are understood through the macroscopic behaviour of molecules. The dipole orientation of conjugated polymers strongly correlates birefringence and produces the corresponding anisotropy of the thin polymer film with a liquid crystalline phase.[20] In particular, the order parameter of mesogenic luminophores aligned by the rubbing process is directly related to the degree of LP emission.[21]

Molecular ordering in the mesogenic luminophore can be easily controlled by a surface treatment such as the rubbing process.[22,23] In general, the orientational ordering of the conjugated polymer is induced parallel to the rubbing direction by mechanically rubbing the PI surface at the interface with the conjugated polymer. The degree of molecular ordering was controlled by adjusting the contact distance between the rubbing roller and the PI layer from 0 to 40 μm. It should be noted that the large contact distance gives rise to large anchoring strength and thus high molecular ordering since the rubbing cloth strongly contacts the PI surface. Fig. 2a and b show the AFM images and the corresponding Fourier transformation images (insets) of the PI surfaces rubbed by 0 and 40 μm contact distances, respectively. The Fourier transformation images clearly confirm that the rubbing process with a contact distance of 40 μm forms an anisotropic morphology along the rubbing direction but the zero-contact rubbing process still retains the isotropic morphology without any preference in the azimuthal direction. With increasing contact distance, the azimuthal symmetry is broken, and the directional preference gives rise to the azimuthal anchoring energy. Fig. 2c and d show the polarizing microscopy textures of the F8BT films coated on
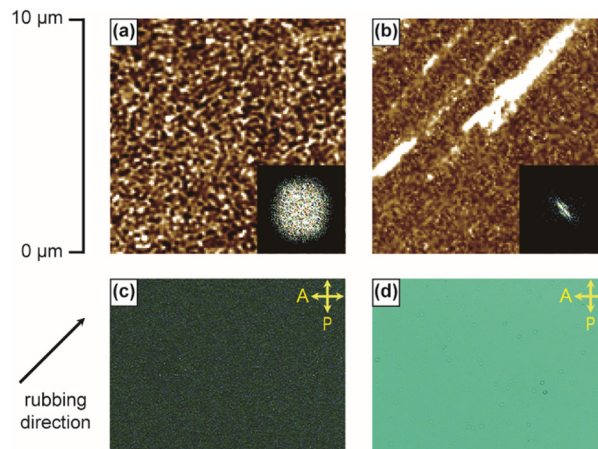

Fig. 2 AFM images and the corresponding fast Fourier-transformed images of surface-treated PI, whose contact distances are (a) 0 μm and (b) 40 μm, respectively. The polarizing microscope textures using crossed polarizers of F8BT on the surface-treated PI, whose contact distances are (c) 0 μm and (d) 40 μm, respectively. Letters "P" and "A" depict the directions of the polariser and the analyser, respectively.

the PI surfaces rubbed with contact distances of 0 and 40 μm, respectively. On the zero-contact rubbed PI layer, the F8BT film presented a dark state under crossed polarizers even though the rubbing direction was rotated by 45° with respect to one of the crossed polarisers (Fig. 2c). On the other hand, on the 40 μm-contact rubbed PI layer, the F8BT film exhibited a bright state under crossed polarisers as shown in Fig. 2d. That is, the F8BT polymers were aligned along the rubbing direction.

The degree of LP emission, corresponding to the order parameter, was investigated by means of the LPPL spectral measurement of the F8BT films prepared with different contact distances since the aligned F8BT emitted LP light along the rubbing direction. Fig. 3a and b show the LPPL spectra and the phase retardation of the 100 nm-thick F8BT film without the chiral dopant on the 40 μm-contact rubbed PI layer. The LPPL spectra were recorded under polarisers parallel ($I_{\parallel}$) and perpendicular ($I_{\perp}$) to the rubbing direction. The polarization ratio (R_P) of the LP light is expressed as an intensity ratio of the parallel component to the perpendicular one of LP light ($R_P = I_{\parallel}/I_{\perp}$) and the corresponding order parameter is written as $S = (R_P - 1)/(R_P + 2)$.[24] In Fig. 3a, the polarization ratio was evaluated to be 12.1 at 546 nm. It should be noted that the polarization ratio depends on the thickness of the EML since the order parameter and birefringence are associated with a penetration distance of an anchoring strength from the alignment layer (AL22636) to the EML.[21] By the measurement of the phase retardation as a function of the rotation angle based on the PEM method,[17] the birefringence (Δn) of the aligned F8BT on the 40 μm-contact rubbed PI layer was evaluated to be 0.62 at 546 nm as shown Fig. 3b. Fig. 3c and d show the order parameter and Δn as a function of contact distance, respectively (see Fig. S3 in the ESI†). In the case of the zero-contact rubbed PI layer, both the order parameter and Δn approach zero since there is no preference in the azimuthal direction on the PI surface. With increasing contact distance,

3302 | *J. Mater. Chem. C*, 2023, **11**, 3300–3305

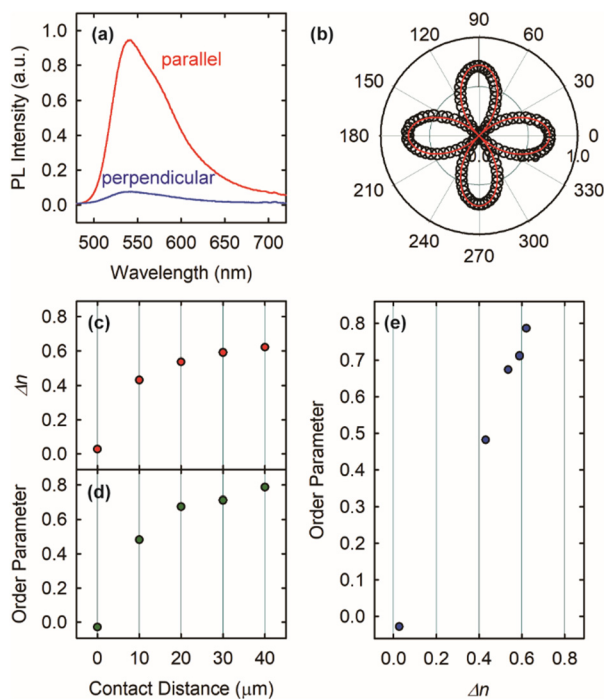This journal is © The Royal Society of Chemistry 2023

Fig. 3 (a) The LPPL spectra of the 100 nm-thick F8BT films without the chiral dopant on the rubbed alignment layer with a contact distance of 40 μm. The spectra were measured using a linear polarizer, both parallel (the red solid curve) and perpendicular (the blue solid curve) to the rubbing direction. (b) The measured phase retardation (symbols) of the sample with a contact distance of 40 μm as a function of the rotation angle using the PEM method. The least-square-fits of the retardation are depicted by the red solid line. (c) Δn and (d) the order parameter as a function of the contact distance. (e) The order parameter–Δn plot from (c) and (d).

the anisotropic morphology along the rubbing direction was formed on the PI layer and mesogenic polymers were aligned along the rubbing direction. Both the order parameter and Δn increased gradually with the increasing contact distance as shown in Fig. 3c and d. Consequently, the order parameter becomes linearly proportional to Δn as shown in Fig. 3e.

Now, we investigate the CP luminescence and the corresponding g factors in both PL and EL devices by introducing the chiral dopant (R5011) with high HTP to the achiral mesogenic polymer (F8BT) with different order parameters. As you already know, no CP luminescence was observed in the mesogenic luminophore without the chiral dopant even at a uniformly aligned EML since no optical phase retardation of the LP light was experienced within the birefringent EML. Furthermore, in the case of the randomly aligned EML, the emitted light is not only unpolarized but also does not experience optical phase retardation; thus, the resultant g value is zero.[7] In the twisted stacks of the mesogenic luminophores, it is assumed that the F8BT film consists of uniformly twisted sublayers and the LP light emitted from an aligned sublayer within the EML experiences the phase retardation and changes to the other polarized light including CP light propagated through the twisted birefringent F8BT.[7,11–14] In the PL process, the LP light is emitted from each sublayer and propagated in the twisted sublayers as

shown in Fig. 1a (left image). On the other hand, in the EP process, the LP light is emitted from an emission zone and propagated toward the anode and the cathode by experiencing the phase retardation. The LP light propagated toward the cathode reflects from the metal cathode and experiences additional phase retardation passing through the entire twisted sublayers as shown in Fig. 1a (right image). Here, since the orientational ordering of F8BT was varied by the contact distance, the emitted LP light is partially polarized, and the degree of LP emission is governed by the polarization ratio and the corresponding order parameter. As a result, the measured dissymmetry g factor, representing the degree of CP emission, is governed by the order parameter. When the partially polarized LP light passes through the film, the measured g value is written as $g = S \cdot g_{ideal}$, where g_{ideal} represents the ideal dissymmetry factor for fully polarized LP light.[7,11]

In the first step, we determined the twisted angles of the F8BT films with different concentrations of the chiral dopant by using Stokes parameters (see Fig. S4 in the ESI†). The chiral dopant plays a predominant role in the helical molecular conformation for CP emission.[25] The twist angles lie within a certain range and increase consistently only by increasing the concentration of the chiral dopant regardless of molecular ordering (see Fig. S5 in the ESI†). Here, in the case of the zero-contact distance, the estimation of the twisted angle was excluded since there was no birefringence.

Next, the ideal dissymmetry g values (g_{ideal}) in the case of fully polarized LP light were calculated as a function of Δn in both PL (g_{PL}) and EL (g_{EL}) processes based on the Mueller matrix analysis at specific twisted angles (see Section 5 in the ESI,† for calculation details). As shown in Fig. 4a and b, the ideal dissymmetry g values were linearly proportional to Δn for various concentrations of the chiral dopant in the case of a perfectly ordered F8BT film. From the linear relationship between the order parameter and Δn as shown in Fig. 3e, the g_{ideal} value is linearly proportional to the order parameter (S). As a result, the measured g value is expressed as the following quadratic equation:

$$g = a \cdot S^2 + g_0,$$

where a represents a fitting coefficient and g_0 implies an extrapolated g value for $S = 0$. Fig. 4c and d show the measured g values (symbols) for various concentrations of R5011 in the PL (g_{PL}) and EL (g_{EL}) devices and the least-square-fits with the quadratic equation of the order parameter. Before evaluating the g values, the circular dichroism (CD) of the twisted F8BT layer was investigated and the dissymmetric g factor of the CP light originated from the resultant CD was negligible[7] (see Fig. S11 in the ESI†). For various concentrations of R5011 (various twisted angles), the fitting parameters are summarized in Table 1 (see Section 6 in the ESI†). Coefficient a has a similar value regardless of the concentration of R5011 since the twisted angle is independent of the order parameter as mentioned in the twisted angle measurement. Interestingly, the extrapolated g_0 values for $S = 0$ gradually increased with increasing concentration of R5011 (twisted angle) as the ideal g values increased

This journal is © The Royal Society of Chemistry 2023

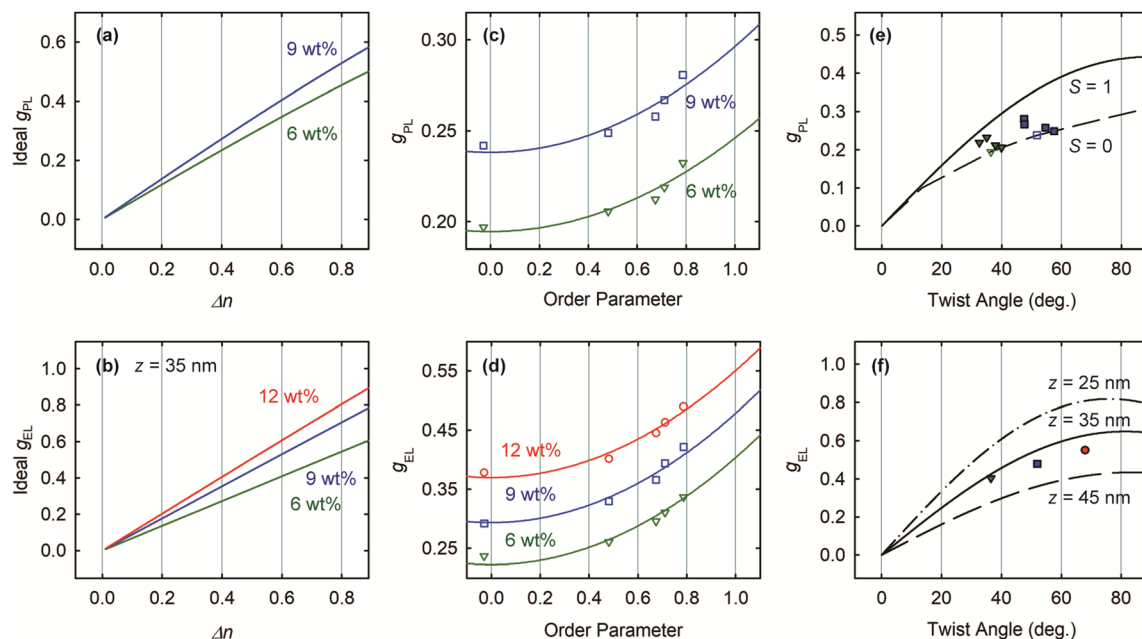*J. Mater. Chem. C*, 2023, **11**, 3300–3305 | **3303**

Fig. 4 The ideal g values in (a) PL and (b) EL devices calculated at a specific twisted angle for various concentrations of the chiral dopant as a function of Δn. Both the ideal g values were linearly proportional to Δn. The measured g values (symbols) for various concentrations of the chiral dopant as a function of the order parameter in (c) PL and (d) EL devices. The solid lines present suitable fits of the experimental data to the quadratic form of the order parameter for various concentrations of R5011 (green triangles for 6 wt%, blue squares for 9 wt%, and red circles for 12 wt%). (e) All PL g values (symbols) measured in (c) as a function of the twisted angle. Triangles and squares present the PL devices with 6 wt% and 9 wt% of R5011, respectively. The same symbols with different twisted angle and g values imply the samples prepared with different contact distances. The solid line depicts the theoretically calculated g values for $S = 1$ (ideally ordered case) and dashed line connects the intercepts ($S = 0$) of the quadratic equation of the order parameter in (c). All PL g values are placed in the boundary region between the two lines. (f) The symbols depict the EL g values measured at different twisted angles, which are governed by the concentrations of R5011. The lines present the calculated EL g values ($S = 1$) for different emission zones.

Table 1 Summary of the quadratic model

Concentration of R5011	Twisted angle	Fitted g_{PL}		Fitted g_{EL}	
		g_0	a	g_0	A
6 wt%	35.60°	0.19	0.05	0.22	0.18
9 wt%	51.74°	0.24	0.06	0.29	0.19
12 wt%	72.66°	—	—	0.37	0.18

with increasing concentration of R5011 at a given Δn (order parameter) as shown in Fig. 4a and b. These results imply that the twisted stacks even at poly-domains are critical rather than the formation of a mono-domain to generate CP light.[7] Furthermore, since there is no retardation for $S = 0$, the anti-reflection condition to eliminate ambient light reflected from the metal cathode in conventional OLEDs is maintained while emitting CPEL with $g = 0.37$ (at 12 wt% of R5011), which leads to the enhancement of luminance efficiency by about 18.5%. Although the actual device efficiency is lower than that in commercialized emission materials, CPEL emission even in the case of $S = 0$ has a significant meaning in improving the efficiency of OLEDs (see Section 6 in the ESI†).

Fig. 4e shows all PL g_{PL} values (symbols) measured in our experiments, the calculated PL g_{PL} value for $S = 1$ (solid line), and the extrapolated PL g_{PL} value for $S = 0$ (dashed line) as a function of the twisted angle. All PL g_{PL} values lie within the boundary

region between the solid and dashed lines. It should be noted that the PL g_{PL} value for $S = 1$ was directly calculated from Stokes parameters after analysing the Mueller matrix without any fitting parameter. The EL g_{EL} values (symbols) averaged over EL devices with various order parameters at the given concentration of R5011 (the given twisted angle) as a function of the twisted angle are shown in Fig. 4f. In the EL process, the EL g_{EL} value was directly calculated by using the Mueller matrix analysis used in the PL process except for the emission zone. The ideal EL g_{EL} values (lines) were calculated for various emission zones as a function of the twisted angle as shown in Fig. 4f. Here, the emission zone (z) is defined as a distance from the TPBi layer (an isotropic medium). Comparing the experimental results and calculations, the emission zone is located at around $z = 35$.

Conclusions

We proposed a simple model describing the dissymmetry g factor in the twisted stacks of mesogenic luminophores depending on their ordering parameter. From careful investigation of the parameters, such as the birefringence and polarization ratio, affecting the g factor under various experimental conditions, we found that the measured PL and EL g values can be expressed as the quadratic equation of the order parameter. Also, it was found and analysed that the g values in the PL and EL processes can be measured in the twisted mesogenic luminophores even when the order parameter

3304 | *J. Mater. Chem. C*, 2023, **11**, 3300–3305

This journal is © The Royal Society of Chemistry 2023

was zero. Such results imply that the twisted stacks even at poly-domains are predominant rather than the formation of a mono-domain to generate CP light. In general, although the twisted mesogenic luminophores on a well-controlled alignment layer produce a high g value, they break the anti-reflection condition to eliminate the reflection of ambient light in conventional OLEDs since they also produce the phase retardation of ambient light. However, since there is no retardation for $S = 0$, the anti-reflection condition is still maintained while emitting CPEL with $g = 0.37$. These results, discussed herein, may help understand the mechanism of CP emission, and enhance the performance of applications based on circular polarization.

Author contributions

C-JY and J-HK designed the experiments. D-ML and G-EK contributed to the experiments. D-ML contributed to the writing – original draft. C-JY contributed to the formal analysis, supervision, and writing – final draft.

Conflicts of interest

There are no conflicts to declare.

Acknowledgements

Notes and references

1 C. Wang, H. Fei, Y. Qiu, Y. Yang, Z. Wei, Y. Tian, Y. Chen and Y. Zhao, *Appl. Phys. Lett.*, 1999, **74**, 19–21.
2 C. Wagenknecht, C.-M. Li, A. Reingruber, X.-H. Bao, A. Goebel, Y.-A. Chen, Q. Zhang, K. Chen and J.-W. Pan, *Nat. Photonics*, 2010, **4**, 549–552.
3 Y. Yang, R. C. da Costa, M. J. Fuchter and A. J. Campbell, *Nat. Photonics*, 2013, **7**, 634–638.
4 D. D. Nuzzo, C. Kulkarni, B. Zhao, E. Smolinsky, F. Tassinari, S. C. J. Meskers, R. Naaman, E. W. Meijer and R. H. Friend, *ACS Nano*, 2017, **11**, 12713–12722.
5 Y. Deng, M. Wang, Y. Zhuang, S. Liu, W. Huang and Q. Zhao, *Light: Sci. Appl.*, 2021, **10**, 76.
6 R. Singh, K. N. N. Unni, A. Solanki and Deepak, *Opt. Mater.*, 2012, **34**, 716–723.
7 D.-M. Lee, J.-W. Song, Y.-J. Lee, C.-J. Yu and J.-H. Kim, *Adv. Mater.*, 2017, **29**, 1700907.
8 K. Saxena, V. K. Jain and D. S. Mehta, *Opt. Mater.*, 2009, **32**, 221–233.
9 S. H. Chen, D. Katsis, A. W. Schmid, J. C. Mastrangelo, T. Tsutsui and T. N. Blanton, *Nature*, 1999, **397**, 506–508.
10 A. Y. Bobrovsky, N. I. Boiko, V. Shibaev and J. H. Wendorff, *Adv. Mater.*, 2003, **15**, 282–287.
11 K. Baek, D.-M. Lee, Y.-J. Lee, H. Choi, J. Seo, I. Kang, C.-J. Yu and J.-H. Kim, *Light: Sci. Appl.*, 2019, **8**, 120.
12 Y.-K. Seo, Y.-J. Lee, J.-H. Kim and C.-J. Yu, *Adv. Opt. Mater.*, 2021, **9**, 2002020.
13 C.-J. Yu, D.-M. Lee, J.-K. Han, Y.-J. Lee, S.-W. Kim, E.-J. Choi and J.-H. Kim, *Adv. Opt. Mater.*, 2022, **10**, 2101674.
14 J.-H. Jung, D.-M. Lee, J.-H. Kim and C.-J. Yu, *J. Mater. Chem. C*, 2018, **6**, 726–730.
15 M. Hamaguchi and K. Yoshino, *Appl. Phys. Lett.*, 1995, **67**, 3381–3383.
16 M. Grell, D. D. D. Bradley, M. Inbasekaran and E. P. Woo, *Adv. Mater.*, 1997, **9**, 798–802.
17 J.-H. Lee, C.-J. Yu and S.-D. Lee, *Mol. Cryst. Liq. Cryst.*, 1998, **321**, 317–322.
18 Y. Zhou, Z. He and S. Sato, *Jpn. J. Appl. Phys.*, 1997, **36**, 2760–2764.
19 P.-G. De Gennes and J. Prost, *The physics of liquid crystals*, Oxford university press, Oxford, 1993.
20 J. Yan, L. Rao, M. Jiao, Y. Li, H.-C. Cheng and S.-T. Wu, *J. Mater. Chem.*, 2011, **21**, 7870–7877.
21 D.-M. Lee, Y.-J. Lee, J.-H. Kim and C.-J. Yu, *Opt. Express*, 2017, **25**, 3737–3742.
22 K. Whitehead, M. Grell, D. Bradley, M. Jandke and P. Strohriegl, *Appl. Phys. Lett.*, 2000, **76**, 2946–2948.
23 S. I. Jo, Y. Kim, J.-H. Baek, C.-J. Yu and J.-H. Kim, *Jpn. J. Appl. Phys.*, 2014, **53**, 03CD04.
24 I. M. Ward, *Structure and properties of oriented polymers*, Applied Science Publishers Ltd, London, 1975.
25 Y. Yang, R. C. da Costa, D. M. Smilgies, A. J. Campbell and M. J. Fuchter, *Adv. Mater.*, 2013, **25**, 2624–2628.